

# Nuclear recoil spectroscopy of levitated particles

Alexander Malyzhenkov,<sup>\*</sup> Vyacheslav Lebedev, and Alonso Castro<sup>†</sup>  
*Chemistry Division, Los Alamos National Laboratory, Los Alamos, NM, USA*  
(Dated: March 14, 2022)

We propose a new method for the detection and characterization of a nuclear decay process. Specifically, we describe how nuclear decay recoil can be observed for small particles levitated in an optical trap with high positional resolution. Precise measurement of the magnitude of each recoil and their rate of occurrence can provide accurate ratios of concentrations of radioactive isotopes. We expect that this new technique for nuclear sample characterization will be especially useful in the area of nuclear forensics.

PACS numbers: 42.50.Wk, 23.60.+e, 23.40.-s, 23.20.Lv

## I. INTRODUCTION

Nuclear decay is a key phenomenon of nature, spanning various fields of scientific study, such as nuclear physics, radiochemistry, radiobiology and medicine. The measurement of radioactivity in a sample, and the determination of the type of emitted radioactive particles is essential for these fields since they allow to characterize the isotopic components of the sample. In principle, knowledge of the decay energy and the emission rate, unambiguously identifies the specific decaying isotope. There are many ways to detect and characterize the products of a nuclear decay: alpha spectrometry, gamma spectrometry, beta detection, scintillation counting, cloud chamber detection, etc. A more general way of sample analysis, mass spectrometry, is also widely used for analysis of nuclear materials, especially for isotopic analysis [1]. Other kinds of methods which do not detect emitted decay particles but instead analyze the sample itself include laser-induced breakdown spectroscopy [2–6], and laser spectroscopy techniques [7, 8].

In this paper, we consider a conceptually different and new approach to nuclear sample analysis by examining the recoil of a daughter particle after each individual decay. Specifically, we consider small particle samples which are difficult to analyze with the above-mentioned methods. Small particle analysis is important for environmental monitoring and especially in nuclear forensics, in which the isotope ratios of nuclear materials present in individual particles are measured in swipe samples taken from the inside and outside of nuclear facilities [1]. We show that, for sub-micrometer particles, the energy of the nuclear decay can be determined very accurately by measuring the recoil of the sample particle levitated in an optical trap. The recoil momentum of the daughter nucleus is fully absorbed by the sample particle resulting in a well defined oscillation in the harmonic potential of the optical trap. We demonstrate that this motion

due to nuclear recoil can be measured by currently available state-of-the-art techniques in optical trapping [9–13]. Moreover, we calculate that an experimental setup similar to those previously described [10, 11] will be able to measure such recoils with high resolution, thus enabling a new method for the characterization of nuclear samples.

In section II we describe the theoretical model behind the micro-particle recoil in an optical trap due to nuclear decay. In section III we explain fundamental and practical limits for the detection of nuclear recoil of an optically trapped particle. In section IV we examine the possibility of using this technique as a nuclear recoil spectrometer. We discuss practical details for the realization of the proposed experiment and potential applications in section V.

## II. THEORETICAL MODEL

Nuclear decay is a fundamental process by which an unstable atom decays into another atom, called the daughter, and emits radiation. This radiation can be carried by  $\gamma$ -photons or by  $\alpha$ - and  $\beta$ -particles. We begin by considering a nuclear decay occurring in an atom of some radioactive material contained within a small solid particle in free space (Fig. 1 (a), (b)). Detection of recoil is only possible if the full momentum kick ( $\mathbf{p}_{n.p.}$ ) from the nuclear particle(s) is transferred to the solid particle ( $\mathbf{p}_{s.p.}$ ). This happens when the solid particle size is such that a nuclear particle ( $\alpha/\beta/\gamma$ ) with kinetic energy ( $E_{kin}$ ) escapes, while the daughter particle remains inside the solid. For example, for  $^{238}\text{PuO}_2$  this condition is satisfied for particle diameters between 10 nm and 10  $\mu\text{m}$  [14]. According to the momentum conservation law, the total momentum of the system before and after the nuclear decay is conserved. Under the assumption that the solid particle was at rest before the decay, we find:

$$\mathbf{p}_{s.p.} = -\mathbf{p}_{n.p.} \quad (1)$$

<sup>\*</sup> Also at the Department of Physics, Northern Illinois University, Dekalb, IL, USA

<sup>†</sup> Corresponding author: acx@lanl.gov

Different decay types ( $\alpha/\beta/\gamma$ ) result in different recoils depending on decay energy, the mass of emitted particle, and the proximity to the relativistic regime. First, we

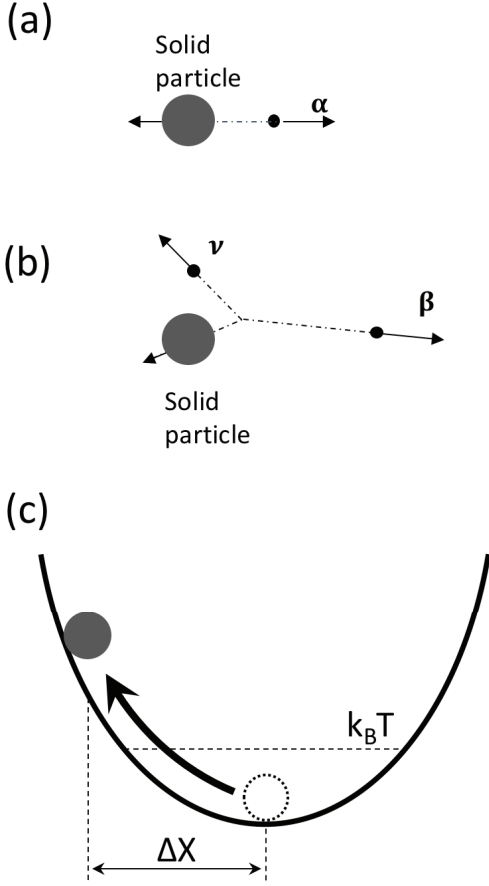
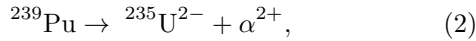
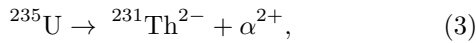


FIG. 1. (a) Schematic picture of  $\alpha$ -decay in a free solid particle: the solid particle with daughter atom (not pictured) recoils in the opposite direction to that of the alpha particle. (b) Schematic picture of  $\beta$ -decay in a free solid particle: a neutrino ( $\nu$ ) and a beta particle initiate recoil of the solid particle. (c) Simplified model of the recoil of the solid particle in an optical trap as a 1D harmonic oscillator.

consider the following examples of alpha decay:



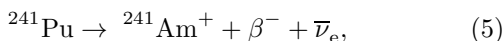
where the  $^{239}\text{Pu}$  half-life is  $\sim 24100$  years, and



where the  $^{235}\text{U}$  half-life is  $\sim 703.8$  million years. The kinetic energy ( $E_{kin}$ ) of an  $\alpha$ -particle in the nuclear decay process in Eq. (2) is  $\sim 5.15$  MeV [15], which is significantly less than its rest mass energy:  $E_{0\alpha} = m_\alpha c^2 = 3.7$  GeV, where  $c$  is the speed of light in vacuum and  $m_\alpha$  is the mass of the  $\alpha$ -particle. For this non-relativistic case, the momentum of the  $\alpha$ -particle is:

$$p_\alpha = m_\alpha V_\alpha = \sqrt{2m_\alpha E_{kin_\alpha}} \quad (4)$$

Another common type of nuclear decay is  $\beta$ -decay. Let us consider the following example:

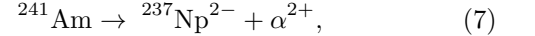


where  $\bar{\nu}_e$  is electron-type antineutrino and the  $^{241}\text{Pu}$  half-life is  $\sim 14.3$  years, while the mean and maximum  $\beta$ -energies for this example are  $\sim 5.2$  keV and  $\sim 20.8$  keV, respectively. Typical kinetic energies of  $\beta$ -particles are in the range 10 keV - 4 MeV, while its rest mass energy:  $E_{0e} = m_e c^2 = 0.511$  MeV, where  $m_e$  is the mass of the electron. For this relativistic case, the momenta of the  $\beta$ -particle and the neutrino are:

$$\begin{aligned} p_\beta &= \gamma \beta m_e c = m_e c \sqrt{\gamma_e^2 - 1}, \\ p_\nu &= m_\nu c \sqrt{\gamma_\nu^2 - 1} \end{aligned} \quad (6)$$

where  $\gamma_{e,\nu} = 1 + \frac{E_{kin_{e,\nu}}}{E_{0_{e,\nu}}}$  are the Lorentz factors for the electron and neutrino, respectively. It is important to note that the neutrino rest mass is very small: the upper limit of the effective Majorana neutrino mass varies in the range 0.061 - 0.165 eV [16]. However, its kinetic energy can be up to a few MeVs, and its continuously distributed momentum leads to continuous energy and momentum spectra of the corresponding  $\beta$ -particle [17, 18].

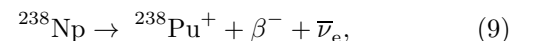
Finally, we consider the case of gamma decay, the process in which an atom emits a  $\gamma$ -photon while transitioning from the excited state to the lower excited or the ground state. For instance, this can happen when  $\alpha$ - or  $\beta$ -decay yield a daughter atom to be in an excited state. For example, the  $\alpha$ -decay of  $^{241}\text{Am}$ :



ends up in the ground state of  $^{237}\text{Np}$  with probability of only 0.37%, while most probably (84.8%), it decays into the excited state (59.54 keV). This  $\alpha$ -decay is followed by the  $\gamma$ -decay almost immediately (67 ns), which results in an additional momentum kick to the solid particle in a random direction. This is under the assumption that the  $\gamma$ -photon leaves the solid particle, which is very likely for micro-particles. The interaction of gamma-rays with matter strongly depends on their energy and the material, so we leave the probability estimates for that process beyond the scope of this paper, while more information can be found in [19]. The kinetic energies ( $E_{kin_\gamma} = \hbar \omega_\gamma$ ) for a massless  $\gamma$ -particle are typically in the range from a few keVs to a few MeVs and are related to its momentum via the linear dispersion relation:

$$p_\gamma = \hbar k_\gamma = E_{kin_\gamma} / c. \quad (8)$$

For the case discussed in Eq. (7), our estimates show that the recoil kick caused by the gamma decay from the most probable excited state of  $^{237}\text{Np}$  (59.54 keV) to the ground state is  $\sim 3.5$  orders of magnitude smaller than the preceding alpha kick. Therefore, for most cases, a gamma kick is negligible when compared to the kick from  $\alpha$ -decay and, hence, can be ignored for practical applications (see sec. IV). In contrast, a  $\beta$ -kick and consequent  $\gamma$ -kick can be of the same order. For instance, beta decay in  $^{238}\text{Np}$  [20]:



results in  $^{238}\text{Pu}$  being in two excited states:  $E_1 = 44.051$  keV and  $E_2 = 1028.542$  keV, with probabilities of 41.1% and 44.8%, respectively [15, 21]. For simplicity, we assume that the neutrino momentum is zero, and the beta particle possesses maximum kinetic energies of 1248 keV and 263 keV, for  $E_1$  and  $E_2$ , respectively. For the first excited level, we find the ratio between  $\beta$ - and  $\gamma$ -kicks to be  $\sim 38$ . The half-life time of  $^{238}\text{Pu}$  on this level is  $\sim 175$  ps, which means that the randomly directed  $\gamma$ -kick will cause spectrum broadening of the  $\beta$ -recoil in this simplified neutrino-less approximation. For the most probable excited level of  $^{238}\text{Pu}$ , our estimates show that the  $\gamma$ -kick is actually  $\sim 1.6$  times larger than the preceding kick from  $\beta$ -decay. To the best of our knowledge, the half-life time at this level has not been measured yet, but if it is less than several  $\mu\text{s}$ , it will significantly complicate beta decay characterization in this particular example. Quantifying  $\beta$ -decay in a solid particle with our method is additionally complicated because of the spectrum broadening due to neutrino emission, so we suppose that the proposed technique is limited to samples where  $\gamma$ -decay is significantly postponed from  $\beta$ -decay, or is not present at all (see sec. IV).

Due to the small size of the particles considered here, it is essential to estimate the rate at which nuclear decay happens, and how it scale with the size of the particle. Nuclear exponential decay is described by the equation:

$$N(t) = N_0 e^{-t/\tau}, \quad (10)$$

where  $N_0$  is the initial number of radioactive atoms,  $N(t)$  is the number of not decayed atoms,  $\tau = t_{1/2}/\ln(2)$  and  $t_{1/2}$  are the mean lifetime and the half-life of the decaying atoms, respectively. The number of nuclear decays per time interval from  $t_1$  to  $t_1 + \Delta t$  can be found as:

$$\Delta N = N(t_1) - N(t_1 + \Delta t) \simeq N(t_1) \Delta t / \tau, \quad (11)$$

if  $\Delta t \ll \tau$ . Therefore, the average recoil rate ( $r = \Delta N / \Delta t$ ) is proportional to the number of radioactive atoms, and inversely proportional to their half-life. In addition, the rate of recoil depends on the isotopic composition of the sample and the radioactivity of each isotope present. For simplicity, consider a solid particle of a radioactive element ( $R$ ) oxide,  $R_A O_B$ , approximated by a sphere with diameter,  $d$ . Then, the mass of this particle is:  $m = \frac{1}{6} \pi \rho d^3$ , where  $\rho$  is the average particle density. Hence, the number of radioactive atoms in this particle is:  $N_R = \frac{m}{M} N_a A$ , where  $N_a$  is Avogadro's number, and  $M$  is the molar mass of the oxide. For example, as presented in Figure 2 (a), for a  $4.5 \mu\text{m}$   $U_3 O_8$  particle with 100%  $^{235}\text{U}$  isotope abundance (half-life  $\sim 703.8$  million years) we find  $r = \frac{N_U \ln 2}{t_{1/2}} = 2$   $\alpha$ -decays per day. In comparison, for  $^{241}\text{Pu}$  (half-life  $\sim 14.3$  years) in a particle of  $\text{PuO}_2$  thirty times smaller ( $d = 150$  nm), we expect  $\sim 4$   $\beta$ -decays per minute.

In order to observe a statistically significant number of recoils, it is essential to localize a particle in space. One

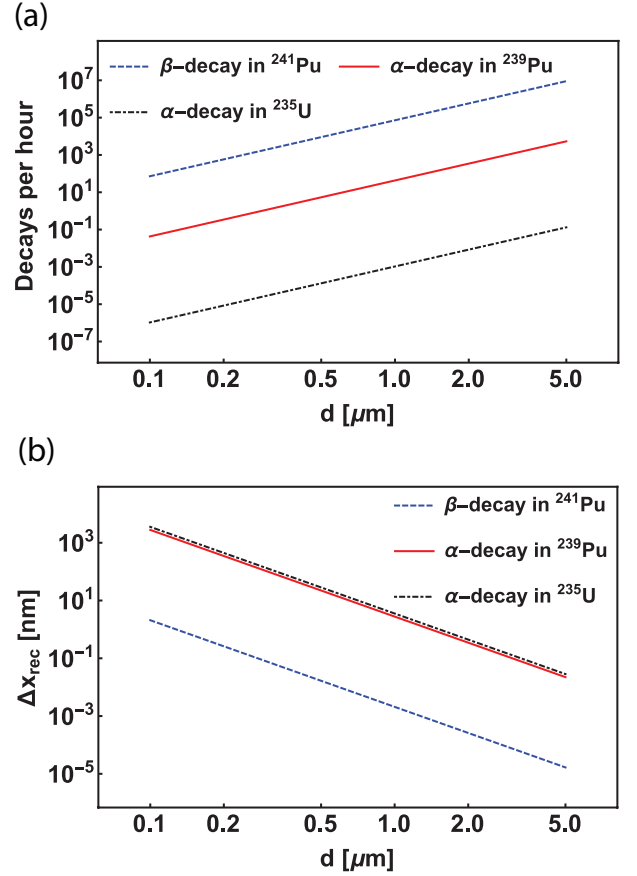


FIG. 2. (a) Recoil rate in the solid particle from its diameter in pure  $^{241}\text{Pu}$  and pure  $^{239}\text{Pu}$  in  $\text{PuO}_2$  particle, and pure  $^{235}\text{U}$  in  $\text{UO}_2$  particle. (b) Deviation of the solid particle in the trap (1 kHz) caused by a nuclear recoil as a function of its diameter. The  $\beta$ -recoil is calculated under the assumption of a zero neutrino momentum and mean  $\beta$ -energy.

of the most advanced methods to achieve this localization is via optical trapping, which allows the levitation of a particle by one or several laser beams [22, 23]. Motion of a solid particle in an optical trap near the point-of-rest is well-described by a harmonic oscillator. Using a 1D approximation we find that the deviation of a particle due to the nuclear recoil is:

$$\Delta x_{\text{rec}} = \frac{V_{s.p.}}{\omega} = \frac{p_{s.p.}}{m_{s.p.} \omega} = \frac{p_{n.p.}}{m_{s.p.} \omega}. \quad (12)$$

As shown above, the deviation caused by nuclear recoil is inversely proportional to the particle mass and, hence, it scales with the diameter of the particle as  $\sim d^{-3}$  (Fig. 2 (b)). For example, for a 100 nm particle of pure  $^{235}\text{U}_3\text{O}_8$  undergoing alpha recoil ( $E_{\text{kin}} \sim 4.5$  MeV) in a trap with  $\omega = 1$  kHz, the expected deviation is  $\sim 1 \mu\text{m}$ . This deviation is well above the positional resolution of recently demonstrated experimental techniques, which are capable of detecting displacements of several picometers [10, 11].

In principle, nuclear decay can happen at any loca-

tion within the solid particle. If it does not happen at the center-of-mass (COM) position, the solid particle will start rotating. However, the dispersion relation,  $E_{kin}(p_{n.p.})$  of a given nuclear particle, which we assume leaves the solid particle without any interaction, as well as the momentum conservation, are not affected by the solid particle rotation and, hence, our mathematical formalism described above still holds. This means that by measuring the deviation of the solid particle with known mass ( $m_{s.p.}$ ) in an optical trap with specific frequency ( $\omega$ ), we can reconstruct the momentum and the energy of the nuclear particle produced in the process of nuclear decay.

### III. PRACTICAL AND FUNDAMENTAL LIMITS FOR RESOLVING NUCLEAR RECOIL

A trapped particle interacts with its surrounding gas via collisions. At thermal equilibrium, the average energy of the COM motion in the trap is  $\sim k_B T$ , where  $T$  is the temperature of the surrounding gas and  $k_B$  is the Boltzmann constant. The Brownian motion of the trapped particle plays the role of positional noise with amplitude:  $\Delta x_{bath} = \sqrt{\frac{k_B T}{m_{s.p.} \omega}}$ . For a  $^{239}\text{PuO}_2$  particle, Figure 3 (a) illustrates how this noise limits the detection of recoils for large particles. Note that for particles less than 60 nm, recoils can be detected due to the following reason. While both the displacements due to nuclear recoil kicks, as well as kicks from the background gas, equally depend on the frequency of the trap, they scale differently with the particle mass,  $1/m_{s.p.}$  and  $1/\sqrt{m_{s.p.}}$ , respectively. The observation of the recoil for such small particles requires a long acquisition time (see Fig. 2 (a)), unless one targets isotopes of high radioactivity.

Since thermal noise obscures nuclear recoils for large particles, it is essential to isolate such particles from the environment by removing air to high vacuum levels, and by cooling their COM motion via active positional feedback [10, 11]. The active feedback cooling is based on applying additional radiation pressure to the trapping beam in order to compensate against particle displacements caused by collisions with the residual gas. Using this technique, a temperature of  $\sim 1.5$  mK was reached for a  $3 \mu\text{m}$  silica micro-sphere at a trapping frequency of  $\sim 9$  kHz along one of the axes, and a pressure of  $\sim 5 \cdot 10^{-5}$  mbar [10]. It has also been reported that a particle COM temperature of  $\sim 0.1$  mK can be reached with a demonstrated sensitivity of the detection system of  $39 \text{ fm Hz}^{-1/2}$ , upon improvement of the cooling technique. In fact, this technique is limited in practice by the resolution of the detector used to measure the particle displacement and its instantaneous velocity, and fundamentally by the photon recoil heating from the feedback laser beams. In the Rayleigh regime, when the particle size is smaller than the wavelength of the trapping laser light, the photon recoil limit can be defeated by

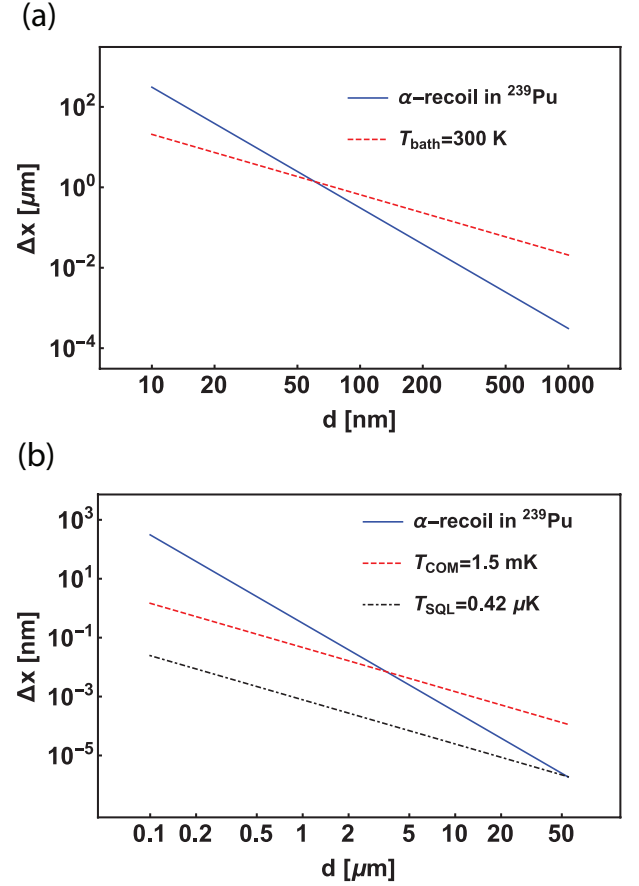


FIG. 3. Optical trap at 9 kHz: (a) The kick from an  $\alpha$ -decay in a  $^{239}\text{Pu}$  sample is compared with the thermal noise at ambient conditions. (b) The kick from an  $\alpha$ -decay in a  $^{239}\text{Pu}$  sample is compared with the amplitude of the COM motion of a particle cooled to  $1.5 \text{ mK}$ , as experimentally demonstrated in [10], and also compared to a particle cooled to the  $T_{SQL}$  of  $0.42 \mu\text{K}$ , rescaled from  $T_{SQL} \sim 5.6 \mu\text{K}$  for a  $120 \text{ kHz}$  trap in [11, 24].

applying a parametric feedback technique [11]. This approach works only for nanoparticles, since it relies on treating the particle as a phase-coherent antennae in the near field regime. Finally, the standard quantum limit (SQL) defines the fundamental cooling limit in an optical trap. This limit is achieved when the uncertainty of the scattered photon momentum is equal to the uncertainty of the measured particle position. If the SQL is reached, the position accuracy scales as  $\Delta x \sim \sqrt{\hbar/(m_{s.p.} \omega)}$  and is independent from the laser power directly [24]. The SQL temperature does not depend on particle mass or size and scales linearly with the trap frequency:  $T_{SQL} \sim \hbar \omega / k_B$ . The fundamental limit sets the lowest achievable temperature of  $\sim 5.6 \mu\text{K}$  for a  $140 \text{ nm}$ -diameter particle at a trapping frequency of  $120 \text{ kHz}$  in ultra-high vacuum of  $\sim 10^{-11}$  mbar, as reported in [11, 24]. Rescaling the SQL temperature to a  $9 \text{ kHz}$  trap yields  $T_{SQL} \sim 0.42 \mu\text{K}$ . Figure 3 (b) compares a typical alpha recoil displacement, average particle motion at the experimentally demon-

strated temperature of 1.5 mK [10, 25], and motion at the fundamental limit, as a function of  $^{239}\text{Pu}$  particle diameter in a 9 kHz trap. This trap frequency can be reached for particles over a wide size range by adjusting the laser parameters and trap configuration. The intersection of the recoil curve with the experimental curve demonstrates that single recoil detection is possible for particles smaller than  $3\text{ }\mu\text{m}$  at experimentally demonstrated temperatures. Moreover, the intersection of the recoil curve with the SQL curve at  $d \sim 50\text{ }\mu\text{m}$ , suggests that a single  $\alpha$ -recoil can be resolved for practically any trappable particle upon reaching the SQL. Theoretical estimates [23, 26–28] demonstrate that COM temperatures close to the quantum-mechanical ground state can be reached experimentally, and many groups are working towards this limit, motivated by studies in non-Newtonian gravitation, Casimir force sensing, measuring vacuum friction, etc. [10, 11, 23, 29–31]. Finally, for particles in the range 100 - 500 nm, the recoil kick is several orders of magnitude larger than the experimentally demonstrated positional noise. This gap is even larger at SQL temperatures. This suggests that a single recoil can not only be detected, but the kinetic energy of the nuclear particle can be reconstructed with good accuracy using the formalism described in Section II, opening up the possibility for resolving the decays of individual isotopes.

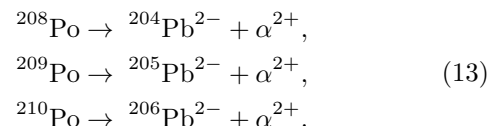
#### IV. NUCLEAR RECOIL SPECTROSCOPY

As discussed above, efficient cooling of the COM motion of a particle decreases its displacements due to Brownian motion to significantly smaller amplitudes than the displacement due to nuclear recoil. However, observation of individual recoils while the particle is under positional feedback is unlikely to be possible, because the feedback will suppress the displacement due to recoil. A more appropriate approach is to switch the feedback off as soon as the particle has been cooled to the lowest temperature, followed by switching the feedback on once the COM temperature is too high to observe the recoil. In the absence of feedback, heating will cause the noise amplitude to grow. Generally speaking, the heating rate is due to collisions with gas molecules  $\Gamma_{gas}$ , photon recoils  $\Gamma_{photon}$  and other experimental noise  $\Gamma_{exp}$ , such as trapping laser noise and mechanical vibrations. In practice,  $\Gamma_{exp}$  dominates the heating rate, providing us with a time window of the order of 0.1-1 seconds [12] to observe the recoil. Since the time it takes to cool the particle is typically much shorter ( $\sim 10\text{ ms}$ ), the duty cycle during which one can observe nuclear recoils is expected to be above 90% for such pulsed sequence. Ultimately, there is a trade off between the duty cycle and the affordable noise level. Since the COM temperature depends linearly on the heating rate at pressures of the order of  $\sim 10^{-5}\text{ mbar}$  [33], this results in a shorter time interval when the feedback is turned off. In contrast, the parametric

feedback damping rate depends quadratically on the positional noise amplitude. Therefore, the effective time to cool down the motion of the particle is practically independent of the upper temperature [32–34]. In other words, in order to decrease the positional noise level, and hence increase the resolution of recoil, one may sacrifice the duty cycle and prolong the observation time.

Measurement of a nuclear recoil with good positional resolution allows to resolve the energies of the emitted decay particles. As mentioned in section III, the COM particle motion plays the role of positional noise for the recoil detection. In the regime, when particle oscillations in the trap are stochastic (Brownian motion), the recoil kick adds to the instantaneous particle motion. Even in the regime when the particle motion is coherent, the decay-initiated recoil still happens with a random phase with respect to the particle oscillation in the trap. Nevertheless, assuming randomly distributed Gaussian noise on the measured recoil kick, we introduce the signal-to-noise ratio (SNR) for the recoil displacement along  $x$ -axis as  $\text{SNR}_x = \Delta x_{rec}/\Delta x_{bath}$ . For alpha decay, the kinetic energy of the  $\alpha$ -particle scales as  $\sim \Delta x_{rec}^2$  according to Eqs. (4) and Eq. (12). For a  $\text{SNR}_x \gg 1$ , using the Taylor series expansion and keeping only linear terms, we find:  $\text{SNR}_\alpha = E_{rec}/\Delta E \simeq 0.5 \cdot \Delta x_{rec}/\Delta x_{bath} \sim m_{s.p.}^{-1/2} \sim \rho^{-1/2} \cdot d^{-3/2}$ , where  $\rho$  and  $d$  are the particle density and the diameter. Figure 4 shows the  $\text{SNR}_\alpha$  as a function of diameter for  $\alpha$ -decay within a  $^{239}\text{PuO}_2$  particle, as described in Eq. (2). The dependence is presented for this particle in the 9 kHz optical trap at different temperatures related to the fundamental limit:  $T_{SQL} = 0.42\text{ }\mu\text{K}$ , and, as demonstrated in [10],  $T_{noise} = 0.1\text{ mK}$ , and  $T_{COM} = 1.5\text{ mK}$  (see section III for details). Figure 4 shows that cooling the motion of the particle to lower temperatures allows to reach higher SNRs, expanding the size range towards larger particles, and hence, allowing the detection of recoil in less radioactive materials. In contrast, at higher temperatures, detecting  $\alpha$ -recoil with good resolution is limited to smaller particles, which requires longer acquisition times.

To ensure adequate acquisition times at the experimentally demonstrated temperature, consider a highly radioactive sample of  $^{209}\text{Po}$  (9%  $^{208}\text{Po}$  and 1%  $^{210}\text{Po}$ ). The half-lives of these isotopes are  $\sim 124\text{ years}$ ,  $\sim 2.9\text{ years}$  and  $\sim 138\text{ days}$ , respectively. Polonium isotopes undergo  $\alpha$ -decay to Pb isotopes according to the equations:



$^{209}\text{Po}$  decays predominantly to the excited level (2.3 keV) and ground level of  $^{205}\text{Pb}$  with probabilities of 79.2 % and 19.7 %, respectively, while both  $^{208}\text{Po}$  and  $^{210}\text{Po}$  decay predominantly to the ground levels of their daughters. Figure 5 shows the  $\alpha$ -energy spectrum, constructed from particle recoil in a 9 kHz trap at different temperatures.

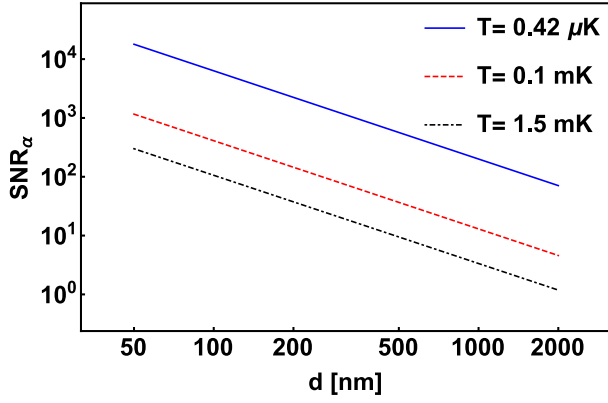


FIG. 4. Signal-to-noise ratio (SNR) for  $\alpha$ -recoil spectroscopy in a 9 kHz optical trap for a  $^{239}\text{PuO}_2$  sample at different temperatures:  $T_{\text{COM}} = 1.5$  mK and  $T_{\text{noise}} = 0.1$  mK demonstrated in [10], and  $T_{\text{SQL}} = 0.42$   $\mu\text{K}$ .

At 1.5 mK [10], the energy peaks for each isotope are well-resolved for a 70 nm particle (Fig. 5 (a)), allowing extraction of isotope ratios. This can be done by integrating the areas under the curves while accounting for the decay rate of each isotope. The average recoil rate is one  $\alpha$ -recoil per  $\sim 26.3$  min for the  $^{209}\text{Po}$  isotope with abundance of 90% in the 70 nm particle. In contrast, a shorter average time is required ( $\sim 3.3$  min) to observe a single  $\alpha$ -recoil in a  $d = 140$  nm particle. However, for a particle of this size at 1.5 mK, the peaks are not resolved (Fig. 5 (b)). At the COM temperature of 0.1 mK (the position detection noise demonstrated in [10]), the peaks are well-resolved for both particle sizes. Finally, upon reaching the SQL temperature (0.42  $\mu\text{K}$ ), it is possible to resolve the nuclear energy structure of  $^{209}\text{Po}$  decay in the 70 nm particle, despite the alpha energies being only  $\sim 2$  keV apart from each other.

The half-life on the excited level of  $^{205}\text{Pb}$  (2.3 keV) is  $\sim 24.2$   $\mu\text{s}$ . The  $\gamma$ -recoil kick is  $\sim 3$  and  $\sim 10$  times smaller than the positional noise at  $T_{\text{SQL}}$  for 70 nm and 140 nm particles, respectively, and therefore, we can ignore the effect of the  $\gamma$ -decay spectrum broadening in the example of Figure 5. However, for very small particles and/or low trap frequencies, the  $\gamma$ -decay broadening can be a dominating effect upon reaching the SQL temperature. Consider two close alpha particle energies:  $E_1$  and  $E_2 = E_1 + \Delta E$ . Assuming that  $\gamma$ -decay happens immediately after  $\alpha$ -decay (on the time scale of the detection system), there could be spectrum broadening, as mentioned in section II. The difference in  $\alpha$ -recoil displacements can be calculated using Eqs. (4) and (12). After linearization ( $\Delta E \ll E_{1,2}$ ) one finds:  $\Delta x_{\alpha_1} - \Delta x_{\alpha_2} \simeq \Delta E \sqrt{2m_\alpha/E_1}/(2m_{s.p.}\omega)$ . Assuming the  $\gamma$ -particle is emitted with energy  $\sim \Delta E$ , or simply that  $\gamma$ -decay in the daughter occurs between these two energy levels, we find the  $\gamma$ -recoil displacement using Eqs. (8) and (12):  $\Delta x_\gamma = \Delta E/(m_{s.p.}\omega c)$ . The ratio

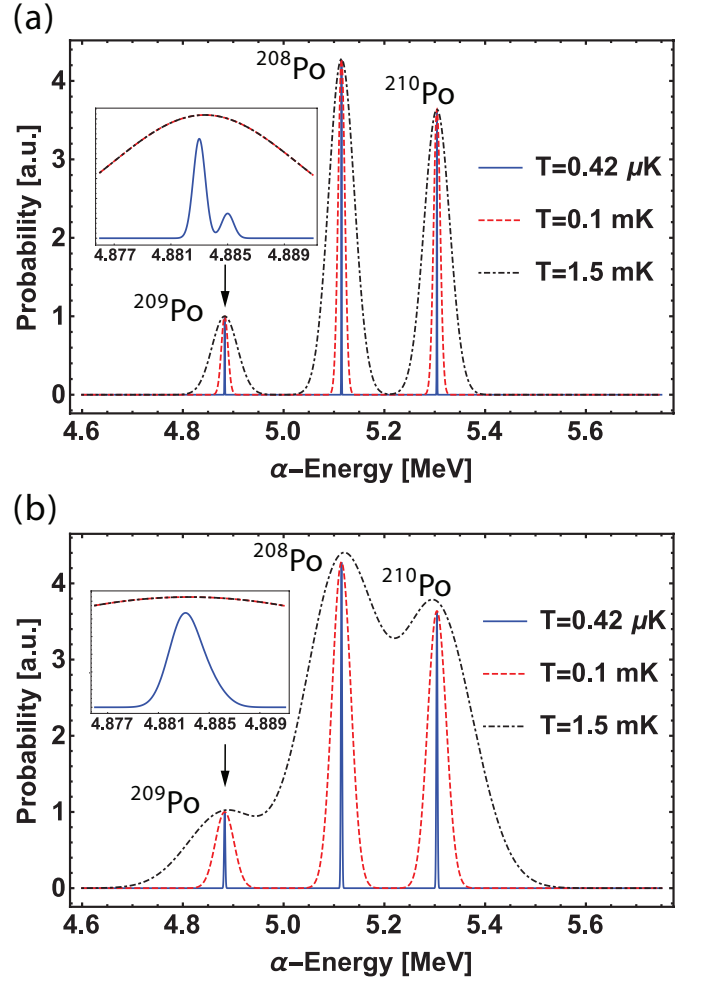


FIG. 5.  $\alpha$ -recoil spectroscopy in the 9 kHz optical trap for the  $^{209}\text{Po}$  (9%  $^{208}\text{Po}$  1%  $^{210}\text{Po}$ ) sample: (a)  $d = 70$  nm and (b)  $d = 140$  nm. The insets demonstrate the resolved (a) and unresolved (b) nuclear energy structure of  $^{209}\text{Po}$  decay:  $\alpha$ -particle kinetic energies of  $\sim 4383$  keV and  $\sim 4385$  keV are related to a daughter ( $^{205}\text{Pb}$ ) being in the excited and ground states, respectively.

$(\Delta x_{\alpha_1} - \Delta x_{\alpha_2})/\Delta x_\gamma \simeq \sqrt{m_\alpha c^2/(2E_1)} \gg 1$ , since the  $\alpha$ -particle rest energy is  $\sim 3.7$  GeV, while typical the kinetic energy is about 5 MeV. Therefore, the  $\gamma$ -kick broadening would not be enough to obscure the nuclear energy structure of the daughter atom.

Upon reaching the SQL temperature in a lower frequency trap,  $\gamma$ -kick can play a significant role in broadening of the spectrum, since it scales as  $(m\omega)^{-1}$ , while the positional noise at  $T_{\text{SQL}}$  scales as  $(m\omega)^{-1/2}$ . Consider a  $^{239}\text{Pu}$  (with 20%  $^{240}\text{Pu}$ ) sample in a 0.9 kHz trap. According to Eq. (2),  $^{239}\text{Pu}$  decays to the excited levels of the daughter ( $^{235}\text{U}$ ):  $E_1 = 0.0765$  keV (70.77%),  $E_2 = 13.04$  keV (17.11%),  $E_3 = 51.7$  keV (11.94%), etc. The half-life of the excited levels are  $\sim 26$  min,  $\sim 500$  ps and  $\sim 191$  ps, for  $E_1$ ,  $E_2$ , and  $E_3$  respec-



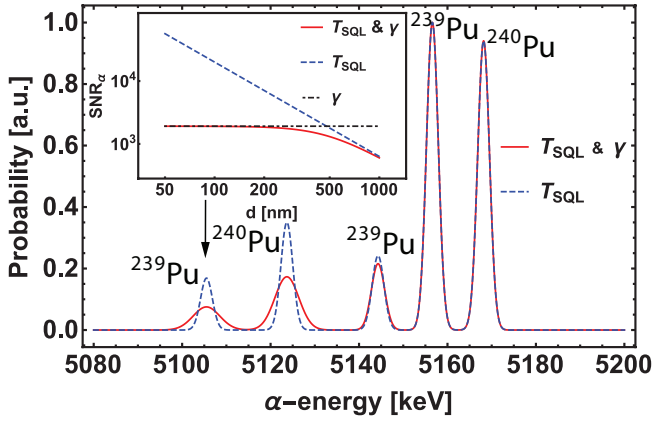
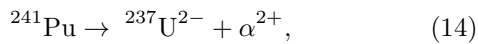


FIG. 6.  $\alpha$ -recoil spectroscopy in a 0.9 kHz optical trap for the  $^{239}\text{Pu}$  (with 20%  $^{240}\text{Pu}$ ) particle ( $d = 300$  nm) at  $T_{\text{SQL}} = 42$  nK with and without  $\gamma$ -kick broadening. Inset demonstrates that the SNR for detecting  $\alpha$ -recoil ( $E_\alpha = 5105.5$  keV) in small particles is dominated by the associated  $\gamma$ -decay ( $E_\gamma = 51.7$  keV).

tively. Similarly,  $^{240}\text{Pu}$   $\alpha$ -decays to the ground (72.8%) and excited,  $E_1 = 45.2$  keV, level (27.1%) of the daughter ( $^{236}\text{U}$ ), where the half-life of the excited level ( $E_1$ ) is 234 ps. Figure 6 shows the alpha spectrum for this sample, constructed in the approximation of only positional noise at  $T_{\text{SQL}} = 42$  nK, and with additionally accounted  $\gamma$ -decay. In this case, the SNR for each  $\alpha$ -peak is calculated individually with and without associated gamma energy. The inset in Fig. 6 shows the SNR for the  $\alpha$ -peak,  $E_\alpha = 5105.5$  keV, calculated in the approximation of only positional noise at  $T_{\text{SQL}}$ , in the approximation of only  $\gamma$ -decay noise, and, when both effects are included. For particles smaller than 200 nm (in a 0.9 kHz trap), the total noise asymptotically approaches to  $\gamma$ -decay noise entering the regime when it is independent from the particle size or trap frequency, since  $\alpha$ - and  $\gamma$ -kicks have a similar dependence on these parameters.

So far, we have discussed the applications of nuclear recoil spectroscopy for samples composed of different isotopes of the same element. Another possible application for this method is getting the ratio of the elements in a sample from the same decay chain, which would allow the determination of the age of the material. For example, consider a recently purified sample of  $^{241}\text{Pu}$  (half-life  $\sim 14.3$  years). It beta-decays to  $^{241}\text{Am}$  with a probability of 99.998% as described in equation (5), and alpha-decays with a probability of only 0.00247%, according to the equation:



The most frequent decay product for  $^{241}\text{Pu}$  is  $^{241}\text{Am}$ , which alpha-decays to  $^{237}\text{Np}$  according to equation (7). Figure 7 (a) presents the  $\alpha$ -decay spectrum, constructed from particle recoil, for a sample of  $^{241}\text{Pu}$  with 1% in-

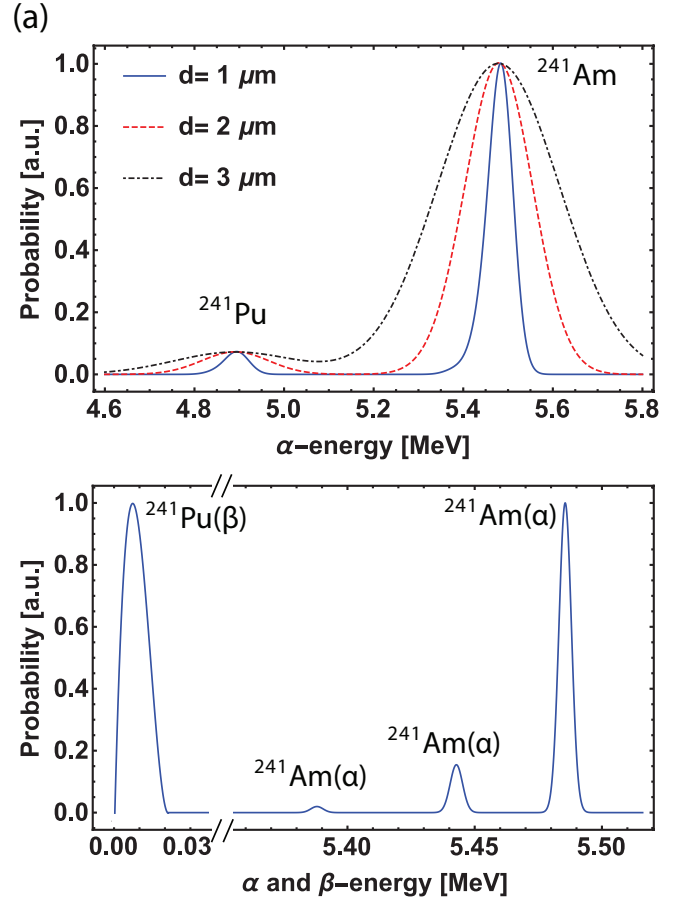


FIG. 7. (a)  $\alpha$ -recoil spectrum for a recently purified  $^{241}\text{Pu}$  (with 1%  $^{241}\text{Am}$ ) sample:  $d = 1 \mu\text{m}$ ,  $d = 2 \mu\text{m}$ ,  $d = 3 \mu\text{m}$ . (b)  $\alpha$ - and  $\beta$ -recoil spectrum for an aged  $^{241}\text{Pu}$  (with 95%  $^{241}\text{Am}$ ) sample ( $d = 0.2 \mu\text{m}$ ). The beta part of the spectrum is plotted in the approximation of massless neutrino, and no distortion by the Coulomb potential.

grown  $^{241}\text{Am}$ , which corresponds to an age of  $\sim 76$  days since last purification. The spectrum is plotted for particles of different sizes, and the widths are defined by the positional noise at  $T_{\text{SQL}} = 0.42 \mu\text{K}$  in a 9 kHz optical trap. It takes on average  $\sim 33$  min,  $\sim 4$  min, and  $\sim 1$  min for  $1 \mu\text{m}$ ,  $2 \mu\text{m}$ , and  $3 \mu\text{m}$  size particles, respectively, for one alpha decay of  $^{241}\text{Pu}$  in this sample to occur. As shown in Fig. 7 (a), the peak widths depend strongly on the particle size. This suggests that selecting a smaller particle is advantageous for obtaining a better resolution, and hence, a better accuracy for extracting the ratio of the isotopes of the sample. On the other hand, in order to obtain proper statistics of the displacements for a short time interval in comparison to the accuracy of the age determination, it would be beneficial to analyze a bigger particle. Therefore, there is a trade-off between the analysis time and energy resolution, which can be mitigated by lowering trap frequencies and cooling the COM motion to lower temperatures.

For comparison, consider an aged sample of  $^{241}\text{Pu}$  with

95%  $^{241}\text{Am}$ , which corresponds to an age of 62 years since last purification. For this sample,  $\alpha$ -decays in  $^{241}\text{Pu}$  are very rare in comparison to  $^{241}\text{Am}$  decays, and therefore, alpha-recoil spectrometry is not able to provide with an accurate isotope composition within a reasonable time. However, our method is capable of measuring both alpha and beta recoils, which is useful for this example, because the half-life in  $^{241}\text{Pu}$  is dominated by beta decay. Figure 7 (b) depicts the combined alpha and beta decay spectrum for this sample for a  $0.2\ \mu\text{m}$  particle at the SQL temperature ( $0.42\ \mu\text{K}$ ) in a 9 kHz trap. Note that the beta peak is asymmetric. For simplicity, it is plotted in the approximation of massless neutrino, ignoring both the distortion by the Coulomb potential [35] and the spectrum broadening due to positional noise. We speculate that the beta spectrum can be reconstructed from the proposed experiment as far as the positional noise ( $\sim 17\ \text{pm}$  at  $T_{SQL}$  in a 9 kHz trap) is less than the recoil displacement ( $\sim 29\ \text{pm}$ ) for a  $\beta$ -particle with mean  $\beta$ -energy (5.2 keV).

## V. DISCUSSION

Having established that it is possible to detect and analyze nuclear recoils in the system that we have proposed here, we turn our attention to other possible applications aside from a nuclear recoil spectrometer. For example, it may now be possible to study plutonium particle migration, which is observed routinely during plutonium metal operations, but has not conclusively explained yet [14]. Specifically, long distance migration of plutonium metal and plutonium oxide particles cannot be explained by recoil alone. It is more likely to be caused by either particle

fragmentation, or evaporation due to the high temperature of the bulk. The experimental setup proposed here may shed light on this topic. With regards to fundamental physics, we speculate that our approach may be of interest to neutrino research. As discussed in section II, the presence of neutrinos can clearly be observed in a beta decay process. Currently, there is a great interest in measuring the neutrino mass [36–38], and searching for neutrino-less double- $\beta$  decay [16, 39, 40]. However, despite the expected high resolution measurements of displacements due to recoil, our proposed system does not detect beta and neutrino emissions independently. An additional way of measuring the energy and momentum of a beta particle would be essential [41].

## VI. CONCLUSION

In this work, we have demonstrated that it should be possible to detect and analyze nuclear decay events in an optically levitated particle. We have pointed out how the sensitivity of this detection system scales with the typical parameters of a realistic experiment. We have also discussed the possible application of this approach to a novel method of nuclear recoil spectroscopy, in particular, of those materials which are of interest to nuclear forensics.

## VII. ACKNOWLEDGMENTS

We thank the Chemistry Division of Los Alamos National Laboratory for providing program development funds, and Dr. Joshua Bartlett for helpful discussions.

- 
- [1] C. G. Lee, K. Iguchi, J. Inagawa, D. Suzuki, F. Esaka, M. Magara, S. Sakurai, K. Watanabe, S. Usuda, J. Radioanal. and Nucl. Chem. **272**, 299 (2007).
  - [2] W. Pietsch, A. Petit, and A. Briand, Spectrochim. Acta B: Atomic Spectroscopy **53**, 751 (1998).
  - [3] F.R. Doucet, G. Lithgow, R. Kosierb, P. Bouchard, and M. Sabsabi, J. Anal. At. Spectrom. **26**, 536 (2011).
  - [4] D.A. Cremers et al., Appl. Spectrosc. **66** 250 (2012).
  - [5] G.C.Y. Chan et al., Spectrochim. Acta B: Atomic Spectroscopy **89**, 40 (2013).
  - [6] G.C.Y. Chan et al., Spectrochim. Acta B: Atomic Spectroscopy **122**, 31 (2016).
  - [7] M.C. Phillips, B.E. Brumfield, N. LaHaye, S.S. Harilal, K.C. Hartig and I. Jovanovic Sci. Rep. **7**, 3784 (2017).
  - [8] V. Lebedev, J.H. Bartlett, A. Malyzhenkov, and A. Castro Rev. Sci. Instr. **88**, 126101 (2017).
  - [9] T. Li, S. Kheifets, D. Medellin, M.G. Raizen, Science **328**, 1673 (2010).
  - [10] T. Li, S. Kheifets, M.G. Raizen, Nature Phys. **7**, 527 (2011).
  - [11] J. Gieseler, B. Deutsch, R. Quidant, L. Novotny, Phys. Rev. Lett. **109**, 103603 (2012).
  - [12] G. Ranjit, M. Cunningham, K. Casey, A.A. Geraci, Phys. Rev. A **93**, 053801 (2016).
  - [13] D.C. Moore, A.D. Rider, and G. Gratta, Phys. Rev. Lett. **113**, 251801 (2014).
  - [14] R.H. Condit, L.W. Gray, M.A. Mitchell, "Pseudo-evaporation of high specific activity alpha-emitting materials", LLNL-CONF-656061 (2014).
  - [15] <https://www-nds.iaea.org/relnsd/NdsEnsdf/QueryForm.html>.
  - [16] A. Gando et al. (KamLAND-Zen Collaboration), Phys. Rev. Lett. **117**, 082503 (2016).
  - [17] C.W. Sherwin, Phys. Rev. **73** (3), 216 (1948).
  - [18] C.W. Sherwin, Phys. Rev. **73** (10), 1173 (1948).
  - [19] G. Nelson and D. Reilly, "Gamma-Ray Interactions with Matter", <http://www.lanl.gov/orgs/n/n1/panda/00326397.pdf>.
  - [20] R.G. Albridge and J.M. Hollander, Nucl. Phys. **21**, 438 (1960).
  - [21] F.E. Chukreev, V.E. Makarenko and M.J. Martin, Nucl. Data Sheets **97**, 129 (2002).
  - [22] A. Ashkin, J.M. Dziedzic, J.E. Bjorkholm, S. Chu, Opt. Lett., **11**, 288 (1986).



- [23] K.C. Neuman and S.M. Block, *Rev. Sci. Instrum.* **75**, 2787 (2004).
- [24] J. Gieseler, B. Deutsch, R. Quidant, L. Novotny, <https://journals.aps.org/prl/supplemental/10.1103/PhysRevLett.109.103603/SupplementaryInformation2.pdf>
- [25] Experimentally reachable COM motion temperature may depend on the particle size, trap geometry, position diagnostic and cooling methods. However, here we simplify that it is independent from the particle size.
- [26] D.E. Chang, C.A. Regal, S.B. Papp, D.J. Wilson, J. Ye, O. Painter, H.J. Kimble, and P. Zoller, *Proc. Natl. Acad. Sci. U.S.A.* **107**, 1005 (2009).
- [27] O. Romero-Isart, M.L. Juan, R. Quidant and J.I. Cirac, *New Journal of Physics* **12**, 033015 (2010).
- [28] Y. Michimura, Y. Kuwahara, T. Ushiba, N. Matsumoto, and M. Ando, *Opt. express* **25** (12), 13799 (2017).
- [29] A.A. Geraci, S.B. Papp, and J. Kitching, *Phys.Rev.Lett.* **105**, 101101 (2010).
- [30] E. Verhagen, S. Delglise, S. Weis, A. Schliesser and T.J. Kippenberg, *Nature* **482**, 63 (2012).
- [31] R. Onofrio, *New J. Phys.* **8** 237 (2006).
- [32] J. Gieseler, R. Quidant, C. Dellago, L. Novotny, *Nat. Nanotechnol.* **9**, 358 (2014).
- [33] E. Hebestreit, R. Reimann, M. Frimmer, L. Novotny, "Measuring the Internal Temperature of a Levitated Nanoparticle in High Vacuum", arXiv:1801.01164 (2018).
- [34] J. Gieseler, L. Novotny, R. Quidant, *Nat. phys.* **9**, 806 (2013).
- [35] Chapter 8 Beta Decay, <http://oregonstate.edu/instruct/ch374/ch418518/Chapter%208%20Beta%20Decay-rev.pdf>
- [36] G. Drexlin, V. Hannen, S. Mertens, C. Weinheimer, *Adv. High Energy Phys.* **2013** (2013).
- [37] S. Mertens, *J. Phys.: Conf. Ser.* **718**, 022013 (2016).
- [38] M. Jerkins, J.R. Klein, J.H. Majors, F. Robicheaux and M.G. Raizen, *New J. Phys.* **12**, 043022 (2010).
- [39] G. Gratta, "Particle physics: Search for neutrinoless double-beta decay", *News and Views, Nature* (Sept 21, 2016) doi:10.1038/nature19473.
- [40] C.E. Aalseth et al. (Majorana Collaboration) *Phys. Rev. Lett.* **120**, 132502 (2018).
- [41] E.W. Otten, *New J. Phys.* **13**, 078001 (2011).